Diels–Alder reaction of vinylene carbonate and 2,5-dimethylfuran: kinetic *vs.* thermodynamic control†

Céline Taffin,[a] Glenda Kreutler,[a] Damien Bourgeois,*[a] Eric Clot[b] and
Christian Périgaud[a]

The Diels–Alder reaction between 2,5-dimethylfuran and vinylene carbonate was studied, both from an experimental and a theoretical point of view. The system was shown to slowly reach a thermodynamic equilibrium, characterized by the almost exclusive formation of the *exo* isomer. We rationalized these results by a comparison with classical systems involving maleic anhydride, and highlighted the different reactivity of vinylene carbonate as a dienophile. Finally, a preparative scale synthesis of pure *exo* isomer **4**, a potentially useful synthon, ensued from this work.

Introduction

The [4 + 2] cycloaddition between a 1,3-diene and an olefin, known as the Diels–Alder reaction, is one of the most useful reactions in organic chemistry.[1] Its synthetic utility lies in the availability of a large number of dienes and dienophiles which can participate in the cycloaddition. Thus, many different types of six-membered carbocyclic structures can be built up. Up to four stereocenters can be formed in a single step, often with high levels of regio- and stereocontrol. Understanding and controlling the stereoselectivity in the installation of these asymmetric centers constitutes a prominent goal in organic chemistry.

The reactions involving furans as dienes are valuable processes,[2] yielding oxanorbornenes that are important intermediates in the synthesis of numerous complex molecules.[3] With this class of compounds, one of the most important aspects of the Diels–Alder reaction is the understanding of the factors influencing the *exo/endo* diastereoselectivity. Alder noticed rapidly that the *endo* product is formed preferentially,[4] and this remains generally observed in many cases. On the other hand, the reaction of furan with maleic anhydride was shown later to lead to the exclusive formation of the *exo* adduct,[5] contrary to Alder's initial assumption.

Extensive efforts have been made to understand the reasons for this exception, and it appeared that the thermodynamic control of the reaction rapidly takes place, favouring the formation of the *exo* adduct, whereas at the first instants of the reaction there is still a kinetic preference for the *endo* adduct.[6] Indeed, the reverse Diels–Alder reaction has a higher rate than the forward reaction, as a consequence of the stability of the starting materials. The aromaticity of the furan heterocycle is lost during the cycloaddition process, rendering the cycloaddition process less favourable compared to other dienes such as butadiene or cyclopentadiene. The experimental kinetic studies were enriched with computational results, including DFT calculations, but the origin of the *exo* selectivity is not fully understood.

Apart from the above case, where the low stability of the [4 + 2] adduct overrules the kinetic preference for *endo* stereoisomers, most of the work dedicated to the selective preparation of *exo* stereoisomers focused on modifications of the reaction partners to destabilize the *endo* transition state.[7] Thus, judicious steric hindrance on dienes or dienophiles can lead to high *exo* stereocontrol of the cycloaddition. The major drawback lies in the numerous steps needed for the synthesis of the suitable reaction partners.

During our synthetic studies towards nucleoside analogues, we devised a route based on a Diels–Alder reaction with vinylene carbonate as dienophile.[8] Use of the latter is not very common, although it leads to highly substituted cyclohexenes or oxanorbornenes, which are precursors to the synthesis of natural products and analogues, such as conduritols[9] and inositols.[10] These syntheses are all based on the reaction with furan. Perhaps further development was limited by the low stereocontrol of the cycloaddition: the *endo* isomer is formed with a modest selectivity (maximum 4.6/1). Also, separation of the isomers is compulsory, either straight after the Diels–Alder reaction, or later in the synthesis, and yields are moderate (maximum 24%).

To reach the desired substitution pattern, we reacted 2,5-dimethylfuran **1** with vinylene carbonate **2** (Scheme 1). As described in the literature,[11] under thermal activation, two diastereomers are produced, the *endo* adduct **3** and the *exo* adduct **4**, in a 40/60 ratio. The selectivity is moderate, and opposite to the reaction with unsubstituted furan. To circumvent the selectivity issue, the reaction sequence we

[a] *Institut des Biomolécules Max Mousseron (IBMM) UMR 5247 CNRS-UM 1-UM 2, Université Montpellier 2, CC 1705, Place Eugène Bataillon, 34095 Montpellier Cedex 5, France. E-mail: damien.bourgeois@univ-montp2.fr; Fax: +33 (0)4 67 04 20 29; Tel: +33 (0)4 67 14 38 79*
[b] *Institut Charles Gerhardt, CNRS 5253, Université Montpellier 2, CC 1501, Place Eugène Bataillon, 34095 Montpellier Cedex 5, France. E-mail: eric.clot@univ-montp2.fr; Fax: +33 (0)4 67 14 48 39; Tel: +33 (0)4 67 14 46 11*
† Electronic supplementary information (ESI) available: ^{1}H and ^{13}C NMR spectra for all new compounds, Cartesian coordinates of optimised structures. See DOI: 10.1039/b9nj00536f
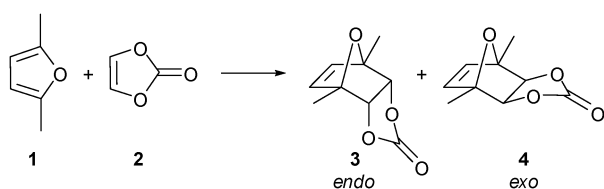
Scheme 1 Diels–Alder reaction between 2,5-dimethylfuran (**1**) and vinylene carbonate (**2**).

developed is stereoconvergent, as both isomers are useful for the synthesis. Thus, separation is not necessary, the yields are much higher, and the methodology proved its efficiency in the synthesis of new nucleoside analogues.

During our studies, we demonstrated that under certain conditions, the reaction of **1** with **2** could also lead to the *exo* adduct with very good yield and selectivity. Thus *exo* adduct **4** can be efficiently obtained on a preparative scale, and can now be seen as a valuable synthon. The aim of the present article is to describe a combined experimental and computational study of the *endo vs. exo* selectivity of the reaction of **1** with **2**.

Results

Experimental studies

Both compounds **1** and **2** are liquids and miscible, so no other solvent was added, as this is usually the case for bi-molecular Diels–Alder reactions. For economical reasons, as the dienophile is far more expensive than the diene, we decided to run the reaction with a 2/1 2,5-dimethylfuran/vinylene carbonate ratio. This ratio was kept constant all through the study. Not surprisingly, no reaction between both compounds occurs at room temperature, and a minimum temperature of 90 °C is required. Even at this temperature, the reaction is very slow. As the furan boils at 94 °C under atmospheric pressure, we decided to conduct the reactions at higher temperature, in sealed tubes, under autogene pressure.

In a first step, we isolated and characterized both diastereomers: complete data were never published. We separated both isomers with flash chromatography on silica gel, instead of fractional crystallization, which led in our hands to mixtures of diastereomers. The important Rf difference renders this operation easy (see experimental for details). After 24 h heating at 130 °C, adducts **3** and **4** are isolated in 25% and 41% yield, respectively. Configuration of these adducts was fully secured by the following procedure (Scheme 2).
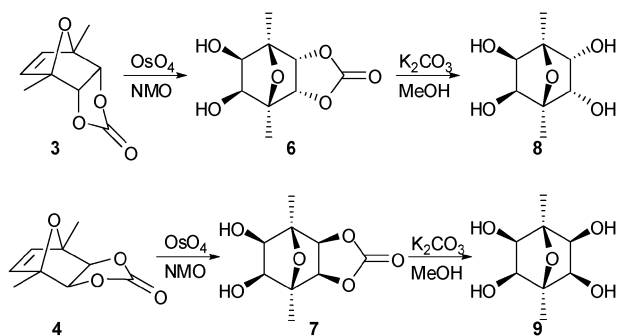
Dihydroxylation of the olefin occurs exclusively *via* the *exo* face of the molecule, in both cases, leading to diols **6** and **7**. Then deprotection of the carbonate moiety with potassium carbonate in methanol leads to tetraols **8** and **9**. The *exo–exo* tetraol **9** presents two symmetry planes, and shows only 3 peaks in its ^{13}C NMR spectrum, whereas the *endo–exo* compound **8** shows 4 peaks.

From the same crude reaction mixture between **1** and **2**, we also isolated bis-adduct **5** in 4% yield (Fig. 1). The formation of such a compound was already mentioned in the first studies of Diels–Alder reactions with vinylene carbonate.[12] It is isolated as a single diastereomer, but its structure was not fully elucidated. A strong nuclear Overhauser effect (nOe) between the protons located at the ring junctions implies that they are all in an axial position. Thus, the bis-adduct derives from the *exo* adduct **4**, *via* an addition of furan **1** from its *exo* side. This side is the least hindered on such systems (see also the dihydroxylation above). The second Diels–Alder addition can again come from an *endo* or an *exo* attack, referring to the furan ring. Both are consistent with the spectroscopic data obtained. The *endo–exo* isomer should, however, be preferred over the *exo–exo* isomer, taking into consideration the closely related works describing the bis-adducts of furan and dimethyl acetylenedicarboxylate.[13]

These first results suggest a very moderate preference for *exo* isomer, in full agreement with the selectivity previously reported (60/40). But when we prolonged the reaction time to increase conversion of starting materials, and thus yields of the cycloadducts, we observed an increase in the *exo/endo* ratio. After heating the same 2,5-dimethylfuran/vinylene carbonate mixture for 48 h at 130 °C, this ratio turned to 3.8/1. And after 4 days, the selectivity was even higher than 8/1. This important change enabled the easy isolation of pure *exo* material directly after crystallisation from AcOEt. A 61% yield was obtained on a multi-gram scale, thus making this route efficient for selective preparation of **4** on a large scale.

These results prompted us to perform a detailed study of the reaction. We clearly demonstrated that, at this temperature, control of the reaction shifts from kinetics to thermodynamics. Running the reaction at 130 °C, and analysing aliquots with ^{1}H NMR at regular time intervals, enabled a quick study of the *exo/endo* ratio of the isomers produced as a function of time (Fig. 2).

The *exo/endo* ratio is close to 1 at the beginning of the reaction, and it slowly and regularly evolves to reach a selectivity greater that 10/1. Heating at 130 °C for 144 h gave an *exo/endo* ratio of 13.2/1, corresponding to a *dr* of 86%. After 216 h (9 days) the ratio stabilized slightly below 15/1,

Scheme 2 Chemical elucidation of relative configurations.
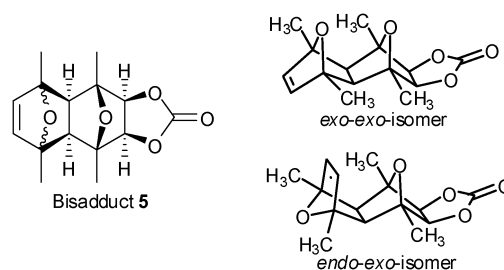
Fig. 1 Possible structures for bis-adduct **5**.
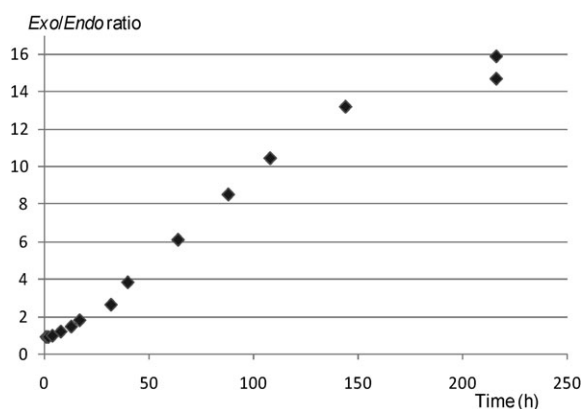
Fig. 2 Time evolution of the *exo/endo* ratio of products during a reaction at 130 °C.

there was no major evolution of the reaction medium, but at this stage the bis-adduct **5** was present in an equivalent amount to the *endo* adduct **3**. Taking into account that the former derives from *exo* adduct **4**, the *exo/endo* ratio, taken as (**4** + **5**)/**3**, becomes 16/1. Quantitative analysis by ^{1}H NMR was also less precise because the peaks broadened slightly. We therefore did not carry on with heating of the reaction medium.

We then performed a quantitative study of the proportions of reagents and products during the reaction, at 110 °C and at 130 °C. We used 1,3,5-trimethoxybenzene (TMB) as an internal standard, and analysed aliquots taken at regular time intervals with ^{1}H NMR. We were able to identify at least one isolated signal for each product (*i.e.* **1**, **2**, **3**, **4** and **5**, plus TMB) in the ^{1}H NMR spectra for quantitative integration (see Fig. 3). We used the signals at 5.83 ppm (**1**, dimethyl furan), 7.13 ppm (**2**, vinylene carbonate), 4.64 ppm (**3**, *endo* adduct), 4.51 ppm (**4**, *exo* adduct), 4.42 ppm (**5**, bis-adduct) and 3.77 ppm (TMB).

During the course of the reaction, we could not see any other methoxy signals that could have originated with side products derived from TMB, the reference is thus stable. The only other signals are multiplets at 0.8, 1.2 and 2.2 ppm, corresponding to degradation products of the furan **1**, which may start to polymerise slowly. They are present only after prolonged heating (more than 144 h), and, as stated before during the *exo/endo* ratio study, analysis of the ^{1}H NMR spectra became more difficult because of peak broadening. Concomitant with the formation of these impurities, the reaction medium turned to black, and became slightly thicker. Thus, the last point used for kinetic analysis is taken at 144 h (6 days).

Quantitative analysis of reaction aliquots enabled plotting of the conversion of **3** and **4** as a function of reaction time (Fig. 4 and 5). Conversion of **3** and **4** corresponds to the quantity of titrated products referred to the quantity of starting dienophile **2** (the limiting reagent). Conversion of **2** is also plotted, and corresponds roughly to the sum of appearing products (**3**, **4** and **5**). This means that no other by-product is formed, at least on an important scale.

Not surprisingly, the reaction performed at 110 °C gives results corresponding to the reaction at 130 °C at shorter
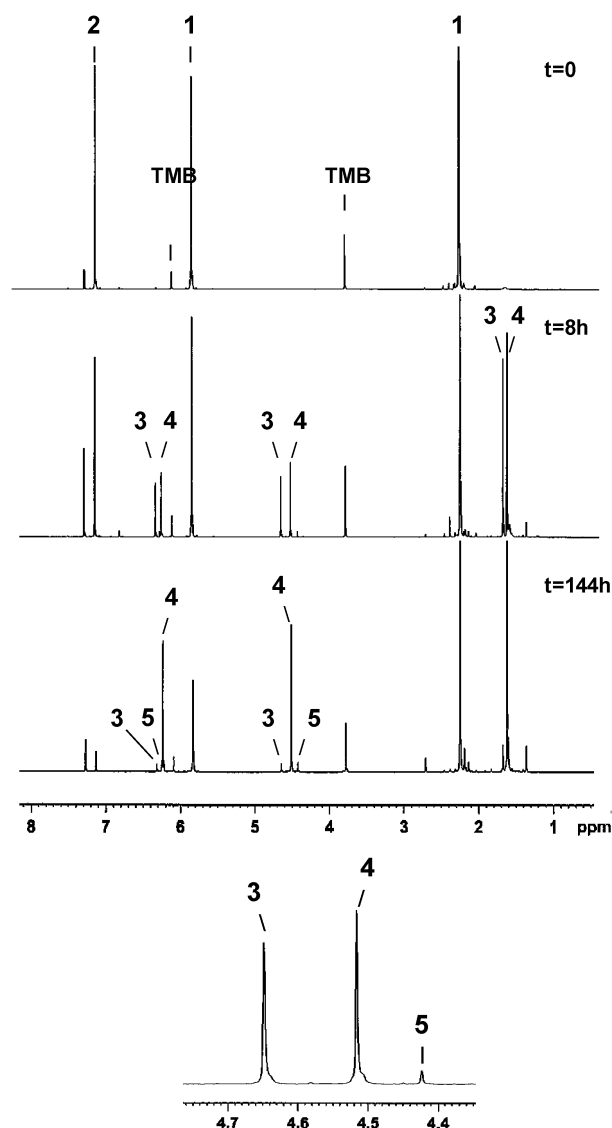
Fig. 3 ^{1}H NMR spectra of aliquots taken at different reaction time at 130 °C.
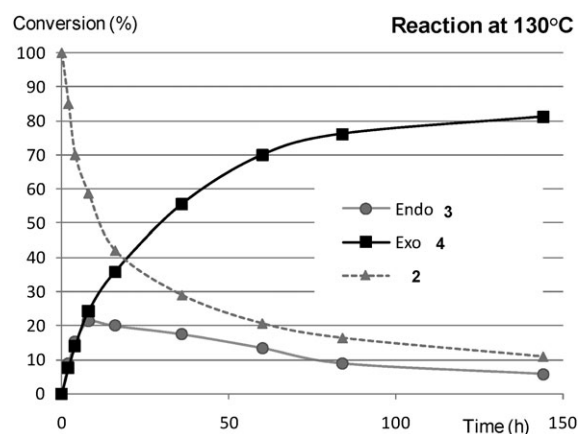
Fig. 4 Conversion of *exo* and *endo* products at 130 °C.

reaction times. Initially, the reaction delivers a 1/1 mixture of *exo* and *endo* adducts, even with a slight preference for
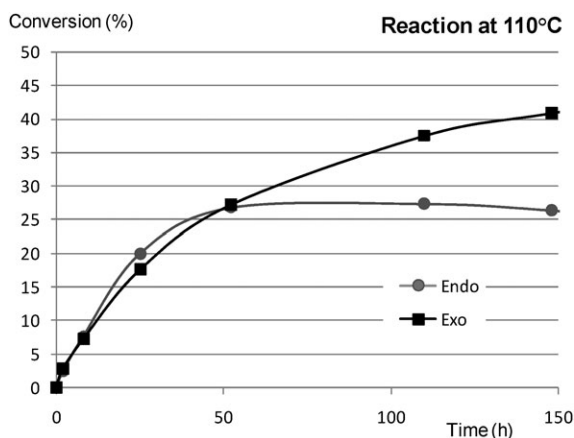
Fig. 5 Conversion of *exo* and *endo* products at 110 °C.

Table 1 Conversion of products during retro Diels–Alder experiments (Detect. means the product is detected, but at a too low level to be quantified)

Reaction		T = 2 h	T = 40 h
3 → 1 + 2	SM (**3**)	4%	32%
	1	6%	29%
	2	4%	27%
4 → 1 + 2	SM (**4**)	<1%	<1%
	1	Detect.	7%
	2	Detect.	4%

endo adduct (*endo/exo* ratio is 1.15 at the very beginning of the reaction). This part ends after *ca.* 50% conversion of starting materials. The second part of the reaction is characterised by a regular disappearance of *endo* adduct **3**, and continuation of the formation of the *exo* adduct **4**. After 6 days heating, there is about 10% **2** remaining, and the presence of bis-adduct **5** in equal amounts to *endo* adduct **3** suggests that secondary reactions may become more important at this stage.

Possibly the system is close to an equilibrium point, as also suggested by the slower evolution of the *exo/endo* ratio during the last part of the reaction (see Fig. 2). To validate this possibility, we showed that at this temperature, both adducts **3** and **4** can undergo retro Diels–Alder reaction.

We encountered difficulties in quantifying precisely the retro Diels–Alder reaction rates. As **1** and **2** are both volatile, a precise titration is difficult, as the head space of the reaction vessel may contain an important proportion of these reagents. Also, at low conversion, as **3** and **4** are solid compounds, the mixture is also solid at room temperature and representative aliquots cannot be taken. Heating **3** or **4** neat (with 3% weight TMB as internal standard) at 130 °C leads to the formation of **1** and **2** as reported in Table 1. The latter products are analyzed after dilution of the whole reaction mixture into CDCl$_3$. In the case of **4**, after 40 h, **1** and **2** are present in 7 and 4% quantity, respectively. We could not quantify the loss of **4**. In the case of **3**, we evaluated the loss of **3** to 4% after 2 h, and 32% after 40 h. These values correspond to the amount of **1** and **2** detected in both cases. We conclude from these results that the reverse reaction takes place during the Diels–Alder reaction of **1** with **2**, with a low rate for **4**, and a high rate for **3**.

The gathered experimental data suggest a comparison with the well known reaction of furan with maleic anhydride. There is also a marked difference with the reaction between vinylene carbonate **2** and unsubstituted furan, which delivers the *endo* adduct. We decided to enrich this experimental study with a computational study, to elucidate the similarities and differences between these systems.

Computational studies

To shed more light on the experimental results, DFT calculations were carried out with the Gaussian03 package.[14] The reactants, transition states and products of the cyclo-addition reactions described in the text were optimized at the B3LYP/6-31G** level.[15] This method has been previously shown to be reliable on Diels–Alder reactions with furans.[16] The computed structures are in very good agreement with the previously reported X-ray structures[17] for **3** and **4** (see Table 4). As Houk mentioned that in certain cases systematic errors can occur,[18] the energies of the various systems were computed at the M05-2X/cc-pVTZ level.[19] This recently developed functional has been shown to yield better energetics.[20] The enthalpy and Gibbs free energy values given in the text are the sum of the M05-2X/cc-pVTZ electronic energy values and the B3LYP/6-31G** thermal corrections at 400 K.

Usually, differences in reactivity for cycloaddition reactions are rationalized in the qualitative framework of FMO theory by looking at the energies of the frontier orbitals, HOMO of the diene and LUMO of the dienophile (Fig. 6). Furans are electron rich dienes, forced into a reactive *cisoid* conformation, with some degree of aromaticity conferred by the delocalisation of the oxygen atom lone pairs into the cycle, creating a 6-π electron system. The reaction of furan (high HOMO) with maleic anhydride (low LUMO) occurs at room temperature, even in solution at moderate concentrations. The same behaviour is observed with cyclopentadiene.

Substitution of furan by methyl groups increases the energy of the HOMO, and 2,5-dimethylfuran **1** can be considered as a 'good' diene, slightly more electron rich than furan. However, the substitution at the 2 and 5 positions has also increased the steric bulk at the reactive sites.[21] On the other hand, one can expect a moderate reactivity of vinylene carbonate, a rather electron rich dienophile as illustrated by the energy of the LUMO (Fig. 6). The cornerstone of FMO theory is the HOMO–LUMO gap between the two reacting molecules and the values in Fig. 6 are consistent with the fact that furan or dimethylfuran need to be heated neat with vinylene carbonate at a minimum of 90 °C for a reaction to occur. However, this qualitative approach cannot account for the
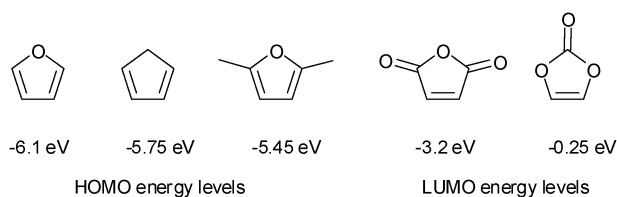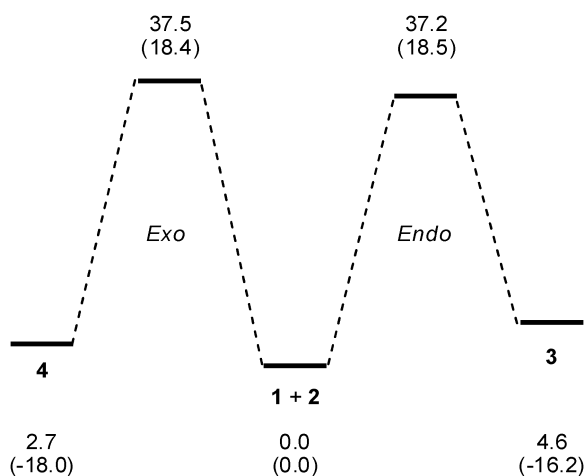

-6.1 eV	-5.75 eV	-5.45 eV	-3.2 eV	-0.25 eV

HOMO energy levels   LUMO energy levels

**Fig. 6** Energy levels of frontier orbitals of selected dienes and dienophiles, obtained from B3LYP/6-31G** calculations.

Fig. 7 Gibbs free energy and enthalpy (in parenthesis) values (kcal mol^{-1}, T = 400 K) for the TS and products of the *exo* and *endo* cycloaddtion reactions relative to **1** and **2**, obtained from M05-2X/cc-pVTZ//B3LYP/6-31G** calculations.

difference in the reported selectivities (*endo vs. exo*) of the reaction between furan or dimethylfuran and vinylene carbonate.

For the reaction between 2,5-dimethylfuran (**1**) and vinylene carbonate (**2**), the reaction profile featuring enthalpy and Gibbs free energy values for formation of the *endo* and *exo* cycloaddition products is shown in Fig. 7.

The transition states were computed using as a guess geometry the results of a computational study for the reaction between furan and maleic anhydride.[16b] Analytical calculations of the vibrational frequencies confirmed the transition state nature of the located extrema. The geometry of the TS (Fig. 8) does not present any striking difference compared to other transition states between cyclic dienes and cyclic dienophiles. The symmetrical nature of the system is reflected in the transition state, where C–C bond formation is synchronous. There is also no major difference between the *endo* and the *exo* transition states. The C–C distances between both partners are 215.9 and 216.0 pm in the *endo* and *exo* systems, respectively.

We also performed similar calculations on the reactions between furan (**10**) and vinylene carbonate, and between dimethylfuran and maleic anhydride (**11**). The Gibbs free energy values (T = 400 K) are reported in Table 2. The most relevant parameters are the relative Gibbs free energy values between the *exo* and *endo* products ($\Delta\Delta G$) and between the *endo* and *exo* TSs ($\Delta\Delta G^{\neq}$).
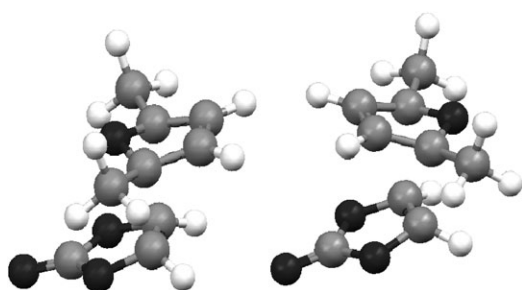
Fig. 8 Structure of *exo* and *endo* transition states.

Discussion

In order to model the observed kinetic profiles of the reaction, we initially took into consideration only the formation of monoadducts **3** and **4**, and assumed that the kinetics are first order (Scheme 3). It is not possible to solve exactly the system of equations resulting from this model because of the presence of terms linking **3** and **4**. We determined the formation constants assuming that, at the beginning of the reaction, the reverse reactions do not take place ([**3**] and [**4**] are very low), and that the system is close to the initial state (*i.e.* [**1**] = [**1**]$_{(t = 0)}$ and [**2**] = [**2**]$_{(t = 0)}$, to remove the correlation between formation of **3** and **4**. The values for the formation constants at 110 and 130 °C are given in Table 3. These values reflect the observed slight preference for the *endo* adduct at the beginning of the reaction (*exo/endo* ratio = 0.9, ie *endo/exo* ratio = 1.1).

Using Eyring's equation, we determined the activation Gibbs free energy at 403 K (130 °C) for the *exo* ($\Delta G^{\#}$ = 35.4 kcal mol^{-1}) and the *endo* adducts ($\Delta G^{\#}$ = 35.3 kcal mol^{-1}). The computed values (Table 2) are in excellent agreement both for the absolute (within 2 kcal mol^{-1}) and relative values.

We then took into account that both reactions are reversible at the temperature of the study. Using the values shown in Fig. 9 for the various rate constants, we could fit the observed data quite well both at the early and late stages of the reaction with data generated from the kinetic model. The values are also in fair agreement with the retro Diels–Alder experiments (k/k_{-1} = 8, **4**; k/k_{-1} = 0.35, **3**). In the case of **3**, the retro Diels–Alder reaction rate estimated from the sole experimental point (see Table 1) gives k_{-1} = 2.0 × 10^{-6} s^{-1}, in the same order of magnitude. The modeled rate constant corresponds to an activation energy of 34.8 kcal mol^{-1} at 403 K, again in excellent agreement with the computed value (within 2 kcal mol^{-1}).

With these values for forward and reverse reaction rate constants, we can estimate the Gibbs free energy for the reaction forming the *endo* and *exo* cycloaddition products (Scheme 4).

The *exo* product is more stable than the *endo* one, in agreement with selective formation of the former upon prolonged heating. The *exo* product is even more stable than the starting reactants, while this is not the case for the *endo* adduct. The calculated values are in qualitative good agreement with the experimental values. Both products are computed to be less stable than the starting reactant but the computed ΔG values for the products are close to that of the reactants (Table 2). More importantly, the *relative* $\Delta\Delta G$ value is computed to be in excellent agreement with the experimental value (2.45 kcal mol^{-1}, exp; 1.9 kcal mol^{-1}, calc.).
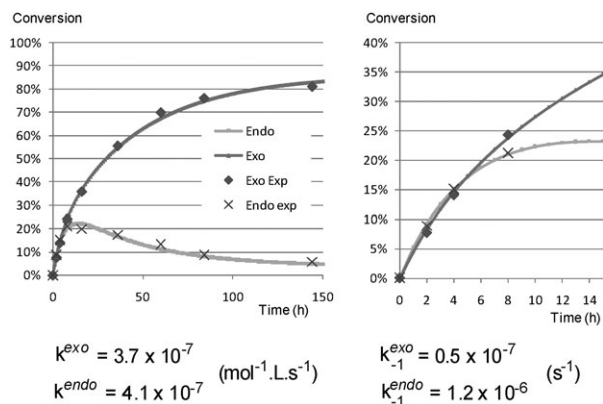
Both experimental and theoretical results indicate that the selectivity originates from a thermodynamic preference for the *exo* isomer. In order to understand the origin of this stability, we examined in detail the structural differences between the computed geometries for **3** and **4**. Moreover, as the X-ray structures for **3** and **4** are available,[17] this allows further test of the accuracy of the computational methodology. In both

Table 2 Gibbs free energies (kcal mol^{-1}, T = 400 K) for various Diels–Alder reactions obtained from M05-2X/cc-pVTZ// B3LYP/6-31G** calculations

Reaction	Exo TS	Exo adduct	Endo TS	Endo adduct	$\Delta\Delta G^{\neq}_{exo/endo}$	$\Delta\Delta G_{exo/endo}$
1 + 2	37.5	2.7	37.2	4.6	+ 0.3	− 1.9
10 + 2	39.3	4.1	38.0	5.7	+ 1.3	− 1.6
1 + 11	27.0	7.7	27.9	7.1	− 0.9	+ 0.6
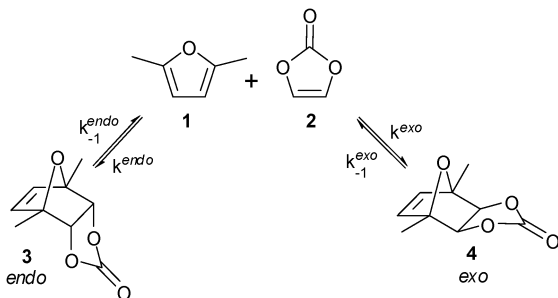
Scheme 3 Simplified kinetic model for the Diels–Alder reaction.

Table 3 Formation rate constants of the Diels–Alder adducts (values are given in mol^{-1} L s^{-1})

	110 °C	130 °C
k^{exo}	0.9 × 10^{-7}	3.7 × 10^{-7}
k^{endo}	1.0 × 10^{-7}	4.1 × 10^{-7}

$$k^{exo} = 3.7 \times 10^{-7}$$
$$k^{endo} = 4.1 \times 10^{-7} \quad (mol^{-1}.L.s^{-1})$$

$$k^{exo}_{-1} = 0.5 \times 10^{-7}$$
$$k^{endo}_{-1} = 1.2 \times 10^{-6} \quad (s^{-1})$$

Fig. 9 Correlation between experimental results (130 °C) and data computed using the kinetic model depicted in Scheme 3.

$$\Delta G = - RT \ln K = - RT \ln \frac{k}{k^{-1}}$$

$$\Delta G_{exo} = -1.65 \text{ kcal.mol}^{-1}$$
$$\Delta G_{endo} = + 0.8 \text{ kcal.mol}^{-1}$$

Scheme 4 Gibbs free energy (T = 403 K) for the reactions forming **3** (*endo*) and **4** (*exo*).

adducts, the cyclic carbonate part of the molecules is almost completely flat. There are only minor differences between **3** and **4**, listed in Table 4.

From these data, slight deformations of the oxanorbornene structure to avoid steric interactions with the carbonate substituent are evidenced. This substituent is moved away from the bridgehead atom in the case of the *exo* isomer (β angle 2° larger), and from the sp^2 carbon atoms in the case

Table 4 Some structural features of adducts **3** and **4** (X-ray values taken from ref. 17, n.d. = not determined)
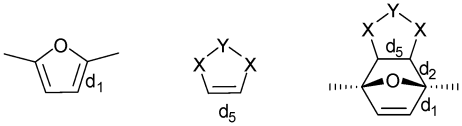

Endo Product (**3**) *Exo* Product (**4**)

	Endo product (**3**)		Exo product (**4**)	
	Calc	X-ray	Calc	X-ray
d_1/pm	152.5	152.2	153.1	153.0
d_2/pm	157.3	156.9	156.7	156.1
d_3/pm	282.5	n.d.	269.7	n.d.
d_4/pm	276.1	n.d.	288.3	n.d.
α	106.8°	107.1°	104.3°	103.6°
β	97.9°	97.6°	100.0°	99.8°
γ	115.6°	114.1°	114.2°	n.d.
δ	111.2°	n.d.	111.8°	110.8

of the *endo* isomer (α angle 2.5–3.5° larger). Probably, the deformation necessary in the *endo* case to completely remove the steric interaction is too important, and thus the d_3 distance (282 pm between an O and a C atom) remains small, compared to the d_4 distance in the *exo* case (288 pm between two O atoms). Furthermore, Van der Waals radii[22] are higher for a C atom (170 pm) than for an O atom (150 pm) rendering the steric interaction in the *endo* isomer (illustrated by d_3) more important than the corresponding interaction in the *exo* isomer (illustrated by d_4).

The lower stability of the *endo* isomer, and its tendency to undergo faster retro Diels–Alder reaction, is reflected by a structure closer to the starting reagents. The distance d_1 is shorter by 0.6 pm, and the distance d_2 is longer by 0.6 pm compared with the *exo* isomer. Also, the distance between the two carbon atoms of vinylene carbonate (d_5) is shortened by 1.3 ppm in the *endo* isomer. These differences are very small, but they all follow the same trend (Table 5).

We examined the potential effects of the methyl substituents, but we did not notice any particular interaction. However, the calculations indicate that the energy difference between the two isomers is 0.3 kcal mol^{-1} smaller in the case of the reaction with unsubstituted furan **10** (Table 2). As stated before, the Diels–Alder reaction between **10** and **2** delivers preferentially the *endo* isomer. The calculations indicate that the kinetic preference for the *endo* product is larger than with 2,5-dimethylfuran ($\Delta\Delta G^{\#}$ = + 0.3 kcal mol^{-1}, **1 + 2**; $\Delta\Delta G^{\#}$ = + 1.3 kcal mol^{-1}, **10 + 2**). The calculated value for $\Delta\Delta G^{\#}$ corresponds to a kinetic ratio between the *endo* and the

Table 5 Comparison between some structural parameters for reagents and products of Diels–Alder reaction of **1** with **2**(top) or **11** (bottom). SM stands for starting materials and n.a. stands for not applicable

Product		d_1/pm	d_2/pm	d_5/pm
$X = O$	SM	136.2	n.a. (∞)	133.1
$Y = C{=}O$	endo (**3**)	152.5	157.3	154.3
	exo (**4**)	153.1	156.7	155.6
$X = C{=}O$	SM	136.2	n.a. (∞)	133.5
$Y = O$	endo	152.8	159.3	153.0
	exo	152.9	159.2	154.1

exo products of *ca.* 5 at 400 K, in excellent agreement with the experimental observations (*endo/exo ca.* 6). However, despite this kinetic bias, the calculations indicate a clear thermodynamic preference for the *exo* isomer. Therefore, we tried to push further the Diels–Alder reaction between **10** and **2**, in order to reach thermodynamic equilibrium.

The results were somehow disappointing. We could reproduce the predominant formation of the *endo* isomer after heating at 130 °C for 12 h. Further heating yielded a very complex mixture, which did not contain the *exo* isomer as the major compound. We also observed that the *endo* isomer was still present. Furthermore, ¹H NMR analysis was hampered by the presence of numerous by products. We assume that furan polymerises more easily than dimethylfuran, and that this system is not adapted to prolonged heating. Also, the autogene pressure is higher with furan, and we are not equipped to run reactions at a higher temperature (pressure reached more than 20 bars at 180 °C).

Finally, we studied as a comparison the reaction between **1** and **11**, a much better dienophile than **2** (Table 2). The computed results are in full agreement with the experimental data reported by Dewar on this reaction.[23] The activation energy is much lower for both *exo* and *endo* adducts, as expected, consistent with the fact that the reaction runs at room temperature. The retro Diels–Alder reaction is also very fast in this case as illustrated by the larger relative energies of the cycloaddition products with respect to separated reactants. The computed data are consistent with the reaction rates determined by Dewar[23] and us. For the *exo* adduct, with **11**, the reverse reaction is about 1.5 fold faster, whereas with vinylene carbonate we found it is almost ten fold slower. We propose that this lower stability is explained by the loss of conjugation occurring when the double bond of **11** reacts. Thus, the Diels–Alder adducts of **1** with **11** show a structure significantly distorted towards the starting materials (Table 5). The d_2 distance is lengthened by 2–2.5 pm, and the d_5 distance shortened by 1.2–1.5 pm in the adducts with **11** compared to **3** and **4**. This striking difference explains why we were able to obtain a very good conversion at a high temperature, and why we encountered no stability issue at room temperature with the *endo* adduct **3**.

Conclusions

We have fully studied the Diels–Alder reaction between 2,5-dimethylfuran **1** and vinylene carbonate **2**. We demonstrated that the reaction can be run under thermodynamic control, to form almost exclusively the *exo* isomer. DFT calculations showed a very good agreement with the experimental results and allowed a rationalization of the reactivity observed. Both experimental and computational approaches are consistent with a slow equilibration at 130 °C, leading to the progressive disappearance of the *endo* isomer, less stable by 2.4 kcal mol⁻¹. The present system differs from the classical reaction between furan and maleic anhydride on two points: (i) the activation energies are higher and the reactions are slower; (ii) the cycloaddition products are more stable relative to separated reactants, so that the equilibrium is shifted towards the *exo* product. Finally, we showed that the *exo* isomer can be easily obtained on a preparative scale after crystallization. Our intention is to pursue our efforts towards the synthesis of new nucleoside analogues, deriving from this useful synthon.

Experimental

General procedures

Unless noted otherwise, all starting materials and reagents were obtained from commercial suppliers and were used without further purification. Tetrahydrofuran was distilled from sodium benzophenone ketyl. Dichloromethane, triethylamine, acetonitrile and pyridine were freshly distilled from calcium hydride. All solvents used for routine isolation of products and chromatography were reagent grade. Reaction flasks were dried at 100 °C. Air and moisture sensitive reactions were performed under argon atmosphere. Flash column chromatography was performed using silica gel 60 (230–400 mesh, Merck) with the indicated solvents. Thin layer chromatography was performed using 0.25 mm silica gel plates (Merck).

Melting points were determined in open capillary tubes on a Büchi-545 and are uncorrected. UV spectra were recorded on an Uvikon 931 (Kontron). Infrared spectra were recorded on a Perkin–Elmer Paragon 1000 FT-IR spectrometer. ¹H NMR and ¹³C NMR spectra were recorded at 300 K on a Bruker 300 Avance and DRX 400, on solutions in the indicated solvent. Chemical shifts are expressed in parts per million (ppm, δ) downfield from tetramethylsilane and are referenced to the residual solvent peak (¹H NMR, CHCl₃ 7.26, DMSO-d_6 2.50) or the deuterated solvent peaks (¹³C NMR, CDCl₃ 77.16, DMSO-d_6 39.52). ¹H-NMR data were reported in the order of chemical shift, multiplicity (s, singlet; d, doublet; m, multiplet and/or multiple resonance), number of protons, and coupling constant in hertz (Hz).

FAB mass spectra were recorded in the positive-ion or negative-ion mode on a JEOL SX 102. The matrix was a mixture (50 : 50, v/v) of glycerol and thioglycerol (G/T). Electrospray (ES) mass spectra and high resolution mass spectra were obtained on a Waters Q-TOF.

Synthesis

Exo **1,7-dimethyl-3,5,10-trioxa-tricyclo[5.2.1.0²,⁶]dec-8-en-4-one (4).** A mixture of 2,5-dimethylfuran **1** (9.8 g, 102 mmol)

and vinylene carbonate **2** (4.4 g, 51 mmol) was heated in a sealed vessel for 72 h at 130 °C. Remaining **1** was distilled off the reaction, then the Diels–Alder adduct was crystallized from AcOEt. The solid was filtered on a sintered glass funnel, then washed with cold AcOEt. *Exo* **4** was obtained as a white solid (5.65 g, 61%). Mp = 114–116 °C; IR (neat) ν/cm^{-1} 2997, 1813, 1368, 1327, 1209, 1162, 1134, 1082, 956; ^{1}H NMR (300 MHz, CDCl$_3$) δ (ppm) 6.22 (s, 2H), 4.51 (s, 2H), 1.58 (s, 6H); ^{13}C NMR (75 MHz, CDCl$_3$) δ (ppm) 155.1, 139.4, 87.2, 80.3, 13.8; MS (ES$^+$) (m/z) 183 [M + H$^+$], 200 [M + NH$_4^+$], 224 [M + CH$_3$CN + H$^+$], 365 [2M + H$^+$]; Anal. calcd for C$_9$H$_{10}$O$_4$ C 59.34, H 5.53, found C 59.30, H 5.28.

Endo **1,7-dimethyl-3,5,10-trioxa-tricyclo[5.2.1.0²,⁶]dec-8-en-4-one (3) and bis-adduct (5).** A solution of 2,5-dimethylfuran **1** (1.115 g, 11.6 mmol) and vinylene carbonate **2** (500 mg, 5.8 mmol) was heated for 24 h at 130 °C. The residue was chromatographed on silica gel with petrol ether–ethyl acetate (70 : 30 then 60 : 40), yielding successively 270 mg (25%) **3** *endo* as a white solid, 438 mg (41%) **4** *exo* as a white solid (total yield: 66%) and 64 mg **5** (4%) as a pale yellow solid.

3: Mp = 109–111 °C; IR (neat) ν/cm^{-1} 2981, 1812, 1798, 1785, 1452, 1386, 1360, 1203, 1181, 1142, 1090, 990; ^{1}H NMR (300 MHz, CDCl$_3$) δ (ppm) 6.30 (s, 2H), 4.63 (s, 2H), 1.66 (s, 6H); ^{13}C NMR (75 MHz, CDCl$_3$) δ (ppm) 154.8, 137.8, 87.1, 81.6, 17.2; MS (ES$^+$) (m/z) 183 [M + H$^+$], 200 [M + NH$_4^+$], 224 [M + CH$_3$CN + H$^+$], 365 [2M + H$^+$]; HRMS (ES$^+$) calcd for C$_9$H$_{11}$O$_4$ (MH$^+$) 183.0657, found 183.0657.

5: Mp = 193–195 °C; IR (neat) ν/cm^{-1} 3078, 2981, 2941, 1807, 1584, 1536, 1454, 1384, 1371, 1346, 1249, 1166, 1114, 1078, 951; ^{1}H NMR (300 MHz, CDCl$_3$) δ (ppm) 6.24 (s, 2H), 4.41 (s, 2H), 2.12 (s, 2H), 1.59 (s, 6H), 1.35 (s, 6H); ^{13}C NMR (75 MHz, CDCl$_3$) δ (ppm) 152.2, 136.1, 84.7, 82.2, 81.3, 54.8, 17.6, 10.1; MS (ES$^+$) (m/z) 279 [M + H$^+$], 296 [M + NH$_4^+$], 320 [M + CH$_3$CN + H$^+$], 557 [2M + H$^+$]; HRMS (ES$^+$) calcd for C$_{15}$H$_{19}$O$_5$ (MH$^+$) 279.1232, found 279.1232.

Endo **8,9-dihydroxy-1,7-dimethyl-3,5,10-trioxa-tricyclo [5.2.1.02,6]decan-4-one (6).** To a cold (0 °C) stirred solution of **3** (250 mg, 1.37 mmol) in a mixture of acetone (3 mL) and water (0.75 mL) was added NMO (260 μL, 1.51 mmol, 60% wt in water), then 0.75 mL of a 0.052 M osmium tetroxide solution in *tert*-butanol. After stirring for 2 h, 5 mL of a Na$_2$S$_2$O$_5$ saturated aqueous solution was added. The mixture was stirred for 30 min, then the solution was extracted with dichloromethane (6 × 20 mL), and the combined organic layers were dried over Na$_2$SO$_4$ and concentrated *in vacuo*. Purification by flash chromatography on silica gel (eluting with methanol–CH$_2$Cl$_2$ 4/96) yielded title compound **6** (201 mg, 68%) as a white solid. Mp = 206–208 °C (dec.); IR (neat) ν/cm^{-1} 3462, 3340, 3006, 2972, 2932, 1785, 1364, 1159, 1080, 1016, 910; ^{1}H NMR (300 MHz, DMSO-d$_6$) δ (ppm) 4.98–4.95 (m, 2H), 4.73 (s, 2H), 3.74–3.71 (m, 2H), 1.35 (s, 6H); ^{13}C NMR (75 MHz, DMSO-d$_6$) δ (ppm) 154.4, 86.3, 80.9, 69.9, 14.8; MS (ES$^+$) (m/z) 217 [M + H$^+$], 239 [M + Na$^+$], 258 [M + CH$_3$CN + H$^+$], 433 [2M + H$^+$], 455 [2M + Na$^+$]; Anal. calcd for C$_9$H$_{12}$O$_6$ C 50.00, H 5.59, found C 49.91, H 5.76.

Exo **8,9-dihydroxy-1,7-dimethyl-3,5,10-trioxa-tricyclo [5.2.1.02,6]-decan-4-one (7).** The same procedure described above for **6** starting from **4** yielded **7** as a white solid with 73% yield. Mp = 240–242 °C (dec.); IR (neat) ν/cm^{-1} 3445, 3367, 2999, 2950, 2913, 1792, 1774, 1376, 1169, 1065, 833; ^{1}H NMR (300 MHz, DMSO-d$_6$) δ (ppm) 4.97 (d, J = 4.2, 2H), 477 (s, 2H), 3.63 (d, J = 4.2, 2H), 1.22 (s, 6H); ^{13}C NMR (75 MHz, DMSO-d$_6$) δ (ppm) 154.4, 87.0, 81.6, 70.6, 10.7; MS (ES$^+$) (m/z) 217 [M + H$^+$], 258 [M + CH$_3$CN + H$^+$], 280 [M + CH$_3$CN + Na$^+$], 433 [2M + H$^+$]; HRMS (ES$^+$) calcd for C$_9$H$_{13}$O$_6$ (MH$^+$) 217.0712, found 217.0711.

Endo **1,4-dimethyl-7-oxa-bicyclo[2.2.1]heptane-2,3,5,6-tetraol (8).** To a stirred solution of **6** (40 mg, 0,18 mmol) in methanol (1 mL) was added K$_2$CO$_3$ (51 mg, 0.37 mmol). After stirring for 3 h, the reaction mixture was filtered on cotton and concentrated *in vacuo*. Purification by flash chromatography on silica gel (eluting with methanol–CH$_2$Cl$_2$ 5/95) yielded title compound **8** (25 mg, 73%) as a white solid. Mp = 169–171 °C; IR (neat) ν/cm^{-1} 3465, 3351, 2994, 2976, 2941, 2905, 1445, 1328, 1254, 1202, 1166, 1150, 1108, 1068, 937, 845, 840; ^{1}H NMR (300 MHz, DMSO-d$_6$) δ (ppm) 4.71–4.70 (m, 2H), 4.39–4.37 (m, 2H, 3.94–3.92 (m, 2H), 3.45–3.43 (m, 2H), 1.17 (s, 6H); ^{13}C NMR (75 MHz, DMSO-d$_6$) δ (ppm) 86.5, 72.5, 69.7, 15.3; MS (ES$^+$) (m/z) 191 [M + H$^+$], 208 [M + NH$_4^+$], 213 [M + Na$^+$], 232 [M + CH$_3$CN + H$^+$], 381 [2M + H$^+$], 403 [2M + Na$^+$]; HRMS (ES$^+$) calcd for C$_8$H$_{15}$O$_5$ (MH$^+$) 191.0919, found 191.0919.

Exo **1,4-dimethyl-7-oxa-bicyclo[2.2.1]heptane-2,3,5,6-tetraol (9).** The same procedure described above for **8** starting from **7** yielded **9** as a white solid with 72% yield. Mp = 209–211 °C; IR (neat) ν/cm^{-1} 3465, 3351, 2994, 2976, 2941, 2905, 1445, 1328, 1254, 1202, 1166, 1150, 1108, 1068, 937, 845, 840; ^{1}H NMR (300 MHz, DMSO-d$_6$) δ (ppm) 4.53 (d, J = 4.7, 2H), 3.45 (d, J = 4.7, 2H), 1.12 (s, 6H); ^{13}C NMR (75 MHz, DMSO-d$_6$) δ (ppm) 87.1, 72.4, 11.4; MS (ES$^+$) (m/z) 191 [M + H$^+$], 213 [M + Na$^+$], 403 [2M + Na$^+$]; HRMS (ES$^+$) calcd for C$_8$H$_{15}$O$_5$ (MH$^+$) 191.0919, found 191.0921.

Procedure for kinetic Diels–Alder experiments

A mixture of 2,5-dimethylfuran **1** (1.23 g, 13 mmol), vinylene carbonate **2** (562 mg, 6.5 mmol) and 1,3,5-trimethoxybenzene (67 mg, 0.4 mmol) was stirred in a screw cap tube for 15 min at 25 °C. An aliquot was taken and used as reference for the initial composition of the reaction mixture. The sealed vessel was then placed at the desired temperature, and heated. Aliquots were taken according to the following procedure: the reaction vessel was cooled to room temperature, and left at this temperature for at least 15 min. 100 μL were taken with a syringe and analysed with ^{1}H NMR in CDCl$_3$. The remaining reaction mixture was closed again and heated.

Notes and references

1 W. Carruthers, *Cycloaddition Reactions in Organic Synthesis*, Pergamon Press, Elmsford, New York, 1990.
2 (a) C. O. Kappe, S. S. Murphree and A. Padwa, *Tetrahedron*, 1997, **53**, 14179–14233; (b) B. H. Lipshutz, *Chem. Rev.*, 1986, **86**, 795–819; (c) F. I. Zubkov, E. V. Nikitina and A. V. Varlamov, *Russ. Chem. Rev.*, 2005, **74**, 639–669; (d) B. A. Keay and

I. R. Hunt, *Aspects of the Intramolecular Diels–Alder Reaction of a Furan Diene (IMDAF) Leading to the Formation of 1,4-Epoxydecalin Systems in Advances in Cycloaddition*, ed. M. Harmata, JAI Press Inc, 1999.

3 P. Vogel, J. Cossy, J. Plumet and O. Arjona, *Tetrahedron*, 1999, **55**, 13521–13642.

4 O. Diels and K. Alder, *Chem. Ber.*, 1929, **62**, 554–562.

5 R. B. Woodward and H. Baer, *J. Am. Chem. Soc.*, 1948, **70**, 1161–1166.

6 (*a*) M. W. Lee and W. C. Herndon, *J. Org. Chem.*, 1978, **43**, 518; (*b*) L. Rulisek, P. Sebek, Z. Havlas, R. Hrabal, P. Capek and A. Svatos, *J. Org. Chem.*, 2005, **70**, 6295–6302; (*c*) Y. Wooi Goh, B. R. Pool and J. M. White, *J. Org. Chem.*, 2008, **73**, 151–156.

7 (*a*) Y. Lam, P. H. Cheong, J. M. Blasco Mata, S. J. Stanway, V. Gouverneur and K. N. Houk, *J. Am. Chem. Soc.*, 2009, **131**, 1947–1957; (*b*) T. S. Powers, W. Jiang, J. Su, W. D. Wulff, B. E. Waltermire and A. L. Rheingold, *J. Am. Chem. Soc.*, 1997, **119**, 6438–6439; (*c*) W. R. Roush and B. B. Brown, *J. Org. Chem.*, 1992, **57**, 3380–3387; (*d*) J. Qi and W. R. Roush, *Org. Lett.*, 2006, **8**, 2795–2798; (*e*) T. Yoon, S. J. Danishefsky and D. De Gala, *Angew. Chem., Int. Ed. Engl.*, 1994, **33**, 853–855; (*f*) T. A. Cernak and J. L. Gleason, *J. Org. Chem.*, 2008, **73**, 102–110; (*g*) B. Boren, J. S. Hirschi, J. H. Reibenspies, M. D. Tallant, D. A. Singleton and G. A. Sulikowski, *J. Org. Chem.*, 2003, **68**, 8991–8995.

8 G. Sautrey, D. Bourgeois and C. Périgaud, *Org. Biomol. Chem.*, 2010, **8**, 378–383.

9 A. Baran, C. Kazaz, H. Secen and Y. Sutbeyaz, *Tetrahedron*, 2003, **59**, 3643–3648.

10 C. R. Kowarski and S. Sarel, *J. Org. Chem.*, 1973, **38**, 117–119.

11 H. J. Knops, K. Steinbeck, P. Babczinski, H. J. Santel and R. R. Schmidt, *German Patent Application*, 3617715, 1987 (DE 3617715).

12 M. S. Newman and R. W. Addor, *J. Am. Chem. Soc.*, 1955, **77**, 3789–3793.

13 J. D. Slee and E. LeGoff, *J. Org. Chem.*, 1970, **35**, 3897–3901.

14 M. J. Frisch, G. W. Trucks, H. B. Schlegel, G. E. Scuseria, M. A. Robb, J. R. Cheeseman, J. A. Montgomery. Jr., T. Vreven, K. N. Kudin, J. C. Burant, J. M. Millam, S. S. Iyengar, J. Tomasi, V. Barone, B. Mennucci, M. Cossi, G. Scalmani, N. Rega, G. A. Petersson, H. Nakatsuji, M. Hada, M. Ehara, K. Toyota, R. Fukuda, J. Hasegawa, M. Ishida, T. Nakajima, Y. Honda, O. Kitao, H. Nakai, M. Klene, X. Li, J. E. Knox, H. P. Hratchian, J. B. Cross, V. Bakken, C. Adamo, J. Jaramillo, R. Gomperts, R. E. Stratmann, O. Yazyev, A. J. Austin, R. Cammi, C. Pomelli, J. W. Ochterski, P. Y. Ayala, K. Morokuma, G. A. Voth, P. Salvador, J. J. Dannenberg, V. G. Zakrzewski, S. Dapprich, A. D. Daniels, M. C. Strain, O. Farkas, D. K. Malick, A. D. Rabuck, K. Raghavachari, J. B. Foresman, J. V. Ortiz, Q. Cui, A. G. Baboul, S. Clifford, J. Cioslowski, B. B. Stefanov, G. Liu, A. Liashenko, P. Piskorz, I. Komaromi, R. L. Martin, D. J. Fox, T. Keith, M. A. Al-Laham, C. Y. Peng, A. Nanayakkara, M. Challacombe, P. M. W. Gill, B. Johnson, W. Chen, M. W. Wong, C. Gonzalez and J. A. Pople, *GAUSSIAN 03 (Revision C.02)*, Gaussian, Inc., Wallingford CT, 2004.

15 (*a*) A. D. Becke, *J. Chem. Phys.*, 1993, **98**, 5648–52; (*b*) C. Lee, W. Yang and R. G. Parr, *Phys. Rev. B: Condens. Matter*, 1988, **37**, 785–89.

16 (*a*) G. A. Griffith, I. H. Hillier, A. C. Moralee, J. M. Percy, R. Roig and M. A. Vincent, *J. Am. Chem. Soc.*, 2006, **128**, 13130–13141; (*b*) S. Calvo-Losada and D. Suarez, *J. Am. Chem. Soc.*, 2000, **122**, 390–391; (*c*) B.S. Jursic, *Tetrahedron Lett.*, 1997, **38**, 1305–1308; (*d*) E. Goldstein, B. Beno and K. N. Houk, *J. Am. Chem. Soc.*, 1996, **118**, 6036–6043; (*e*) L. R. Domingo, M. J. Aurell, M. Arno and J. A. Saez, *J. Org. Chem.*, 2007, **72**, 4220–4227; (*f*) D. D. Claeys, K. Moonen, B. I. Roman, V. N. Nemykin, V. V. Zhdankin, M. Waroquier, V. Van Speybroeck and C. V. Stevens, *J. Org. Chem.*, 2008, **73**, 7921–7927; (*g*) M. Dadwal, M. K. Kesharwani, V. Danayak, B. Ganguly, S. M. Mobin, R. Muruganantham and I. N. N. Namboothiri, *Eur. J. Org. Chem.*, 2008, 6106–6118.

17 B. Bonnaud, A. J. Tenon, N. Ebby, C. N'Guessian, J. P. Aycard and J. Lapasset, *Acta Crystallogr., Sect. C: Cryst. Struct. Commun.*, 1992, **48**, 150–153. This reference gives no detail regarding the conditions nor the diastereoselectivity of the reaction. Only the X-ray structures are given, without any other spectroscopic data.

18 S. Pieniazek, F. R. Clemente and K. N. Houk, *Angew. Chem., Int. Ed.*, 2008, **47**, 7746–7749.

19 For M05-2X, (*a*) Y. Zhao, N. E. Schultz and D. G. Truhlar, *J. Chem. Theory Comput.*, 2006, **2**, 364–82for cc-pVTZ, (*b*) T. H. Dunning, Jr., *J. Chem. Phys.*, 1989, **90**, 1007–23.

20 Y. Zhao and D. G. Truhlar, *Acc. Chem. Res.*, 2008, **41**, 157–167.

21 In the case of the reaction with fumaronitrile, 2,5-dimethylfuran was found more reactive than furan itself: M. J. Cook and S. J. Cracknell, *Tetrahedron*, 1994, **50**, 12125–12132.

22 A. Bondi, *J. Phys. Chem.*, 1964, **68**, 441–451.

23 M. J. S. Dewar and A. B. Pierini, *J. Am. Chem. Soc.*, 1984, **106**, 203–208.